




Bicyclic γ -amino acids as inhibitors of γ -aminobutyrate aminotransferase

Andrea Pinto, Lucia Tamborini, Eugenia Pennacchiotti, Antonio Coluccia, Romano Silvestri, Gregorio Cullia, Carlo De Micheli, Paola Conti & Daniela De Biase


To cite this article: Andrea Pinto, Lucia Tamborini, Eugenia Pennacchiotti, Antonio Coluccia, Romano Silvestri, Gregorio Cullia, Carlo De Micheli, Paola Conti & Daniela De Biase (2016) Bicyclic γ -amino acids as inhibitors of γ -aminobutyrate aminotransferase, *Journal of Enzyme Inhibition and Medicinal Chemistry*, 31:2, 295-301, DOI: [10.3109/14756366.2015.1021251](https://doi.org/10.3109/14756366.2015.1021251)

To link to this article: <http://dx.doi.org/10.3109/14756366.2015.1021251>

 [View supplementary material](#) 

 Published online: 25 Mar 2015.

 [Submit your article to this journal](#) 

 Article views: 55

 [View related articles](#) 

 [View Crossmark data](#) 

 Citing articles: 1 [View citing articles](#) 

RESEARCH ARTICLE

Bicyclic γ -amino acids as inhibitors of γ -aminobutyrate aminotransferase

Andrea Pinto¹, Lucia Tamborini¹, Eugenia Pennacchietti², Antonio Coluccia³, Romano Silvestri³, Gregorio Cullia¹, Carlo De Micheli¹, Paola Conti¹, and Daniela De Biase²

¹Dipartimento di Scienze Farmaceutiche, Università degli Studi di Milano, Milano, Italy, ²Istituto Pasteur – Fondazione Cenci Bolognetti, Dipartimento di Scienze e Biotechnologie Medico-Chirurgiche, Sapienza Università di Roma, Latina, Italy, and ³Istituto Pasteur – Fondazione Cenci Bolognetti, Dipartimento di Chimica e Tecnologie del Farmaco, Sapienza Università di Roma, Roma, Italy

Abstract

The γ -aminobutyrate (GABA)-degradative enzyme GABA aminotransferase (GABA-AT) is regarded as an attractive target to control GABA levels in the central nervous system: this has important implications in the treatment of several neurological disorders and drug dependencies. We have investigated the ability of newly synthesized compounds to act as GABA-AT inhibitors. These compounds have a unique bicyclic structure: the carbocyclic ring bears the GABA skeleton, while the fused 3-Br-isoxazoline ring contains an electrophilic warhead susceptible of nucleophilic attack by an active site residue of the target enzyme. Out of the four compounds tested, only the one named (+)-**3** was found to significantly inhibit mammalian GABA-AT *in vitro*. Docking studies, performed on the available structures of GABA-AT, support the experimental findings: out of the four tested compounds, only (+)-**3** suitably orients the electrophilic 3-Br-isoxazoline warhead towards the active site nucleophilic residue Lys329, thereby explaining the irreversible inhibition of GABA-AT observed experimentally.

Keywords

3-Br-isoxazoline, docking, GABA, GABA cyclic analogue, PLP-dependent enzyme

History

Received 9 January 2015
Revised 13 February 2015
Accepted 13 February 2015
Published online 25 March 2015

Introduction

Inhibition of neurotransmission in the central nervous system (CNS) is primarily dependent on γ -aminobutyrate (GABA, Figure 1)¹. This molecule plays an important role in the proper functioning of the brain, where relief of GABA inhibition, i.e., disinhibition, has been recognized to be even more important than excitation itself. This is why aberrations of GABAergic neurotransmission, which include decreased GABA synthesis via glutamate decarboxylase (GAD, E.C. 4.1.1.15; the GABA-synthesizing enzyme), altered transport and dysfunction in receptor activity have been implicated in several neurological and psychiatric disorders such as epilepsy, autism, schizophrenia, panic disorder, and pain^{2–6}. Moreover, GABA has been recognized as a trophic factor during early postnatal development of the CNS as well as in adult neurogenesis^{7,8}.

GABA exerts its biological effect through the interaction with ionotropic GABA_A and GABA_C receptors and metabotropic GABA_B receptors^{7,9,10}. GABA is removed from the synaptic cleft by high affinity sodium-dependent GABA transporters located both in neurons and in glial cells, where it is either recycled or degraded^{11,12}. The approaches used to increase/modulate GABAergic transmission include orthosteric and allosteric activation of the GABA receptors and inhibition of GABA re-uptake into neuronal and glial cell bodies. Because to date there are no

activating molecules that selectively enhance the activity of GAD67, the major GAD isoform involved in GABA synthesis in the CNS, an alternative strategy to achieve an increase in GABA levels consists in the effective inhibition of the major GABA-degradative enzyme, i.e., GABA aminotransferase (GABA-AT, E.C. 2.6.1.19)^{13–15}. Both GAD and GABA-AT are pyridoxal 5'-phosphate (PLP)-dependent enzymes, but localized in different compartments, the former in the cytosol and the latter in the mitochondrial matrix.

The anticonvulsant drug Vigabatrin (Figure 1), a structural analogue of GABA, irreversibly inhibits GABA-AT mostly via a Michael addition mechanism, which involves the nucleophilic attack of the Lys329 ϵ -amino group to the distal carbon on the vinyl moiety of Vigabatrin^{16,17}. This residue locates in the active site of GABA-AT, where it forms an imine bond with PLP (internal aldimine) and is probably directly involved in proton abstraction at the α -carbon, the necessary step in promoting Vigabatrin reactivity.

Surprisingly, the GABA cyclic analogue **1** does not inactivate GABA-AT but behaves as a substrate, and this was explained by computer modeling as the result of an improper positioning of the double bond in the ring with respect to the ϵ -amino group of Lys329¹⁸. On the contrary, derivative **2**, characterized by the presence of a difluorovinyl moiety, turned out to be an extremely potent GABA-AT inhibitor, 52 times more potent than Vigabatrin itself, when assayed under suboptimal conditions¹⁵. This result has been accounted for by considering the mechanism of inactivation, which implies the initial formation of an imine adduct between the amine group of **2** and PLP, followed by the

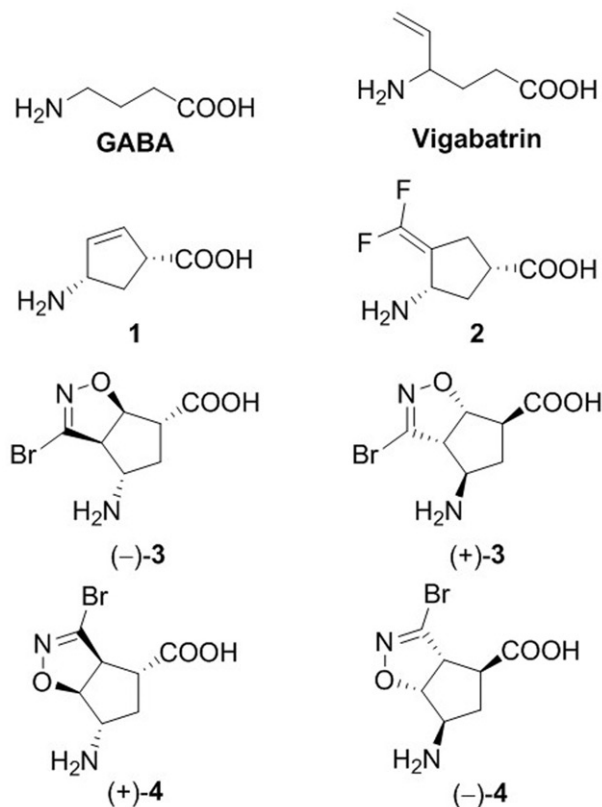


Figure 1. Chemical structures of GABA, Vigabatrin, rigid GABA analogues (**1** and **2**) and the newly designed bicyclic compounds **3** and **4**, described in this work.

nucleophilic attack of Lys329 at the distal carbon of the methylenyl double bond, favored by the presence of two electron-withdrawing fluorine atoms on the double bond itself¹⁹.

Based on the mechanism of action proposed for GABA-AT inhibitors, we designed the novel potential inhibitors **3** and **4**, as depicted in Figure 1. These new compounds are characterized by a bicyclic structure in which the carbocyclic ring bears the GABA skeleton, while the fused 3-Br-isoxazoline ring represents the electrophilic warhead capable to undergo a nucleophilic attack by Lys329 (Scheme 1).

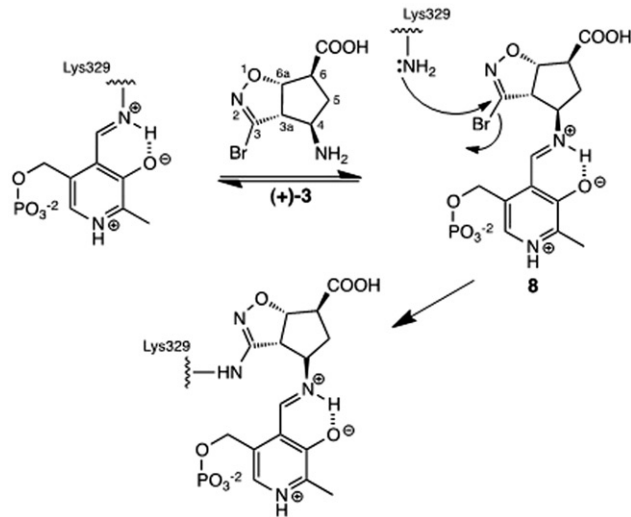
The rationale for using the 3-Br-isoxazoline as a warhead is based on our previous findings showing that the 3-Br-isoxazoline ring can indeed react with a nucleophilic amino acid residue, such as Cys, when the moiety is correctly positioned into the active site of a target enzyme^{20–22}. Moreover, a favorable reactivity of 3-bromoisoxazolines toward amines, to generate the corresponding 3-amino-isoxazolines, has been reported²³. On this ground, we hypothesized the mechanism of inactivation proposed in Scheme 1, in which the 4-amino group forms an imine adduct with PLP, correctly positioning the 3-Br-isoxazoline nucleus for the nucleophilic substitution by the ϵ -amino group of Lys329.

Based on this hypothesis, compounds (–)-**3**, (+)-**3**, (–)-**4**, and (+)-**4** were tested *in vitro* for their ability to inactivate mammalian GABA-AT and the results were rationalized by means of docking studies.

Materials and methods

Chemistry and compounds preparation

All reagents were purchased from Sigma (St. Louis, MO). ¹H NMR and ¹³C NMR spectra were recorded with a Varian Mercury



Scheme 1. Proposed reaction mechanism. To simplify the scheme, only one representative compound, i.e. (+)-**3**, is shown.

300 (300 MHz) spectrometer. Chemical shifts (δ) are expressed in ppm, and coupling constants (J) are expressed in Hz. Rotary power determinations were carried out using a Jasco P-1010 spectropolarimeter (PerkinElmer, Inc., Waltham, MA), coupled with a Haake N3-B thermostat (PerkinElmer, Inc., Waltham, MA). TLC analyses were performed on commercial silica gel 60 F₂₅₄ aluminum sheets; spots were further evidenced by spraying with a dilute alkaline potassium permanganate solution or ninhydrin. MS analyses were performed on a Varian 320-MS triple quadrupole mass spectrometer with ESI source (PerkinElmer, Inc., Waltham, MA). Microanalyses (C, H, and N) of new compounds were within $\pm 0.4\%$ of theoretical values. HPLC analyses were performed with a Jasco PU-980 pump (PerkinElmer, Inc., Waltham, MA) equipped with a UV–vis detector Jasco UV-975 (wavelength: 220 nm) and a KROMASIL 5-AmyCoat column (Agilent Technologies, Santa Clara, CA) ($4.6 \times 250 \text{ mm}^2$). Preparative HPLC was performed with a 1525 Extended Flow Binary HPLC Pump, equipped with a Waters 2489 UV–vis detector (Waters, Milford, MA) and a KROMASIL 5-AmyCoat column ($21.2 \times 250 \text{ mm}^2$, AkzoNobel, Amsterdam, Netherlands) at a flow rate of 20 mL/min.

(3*R*,4*S*,7*R*,7*aS*)-3-Bromo-4,5,7,7*a*-tetrahydro-4,7-methanoisoxazolo[4,5-*c*]pyridin-6(3*aH*)-one (+)-**6** and (3*aS*,4*R*,7*S*,7*aS*)-3-bromo-3*a*,4,7,7*a*-tetrahydro-4,7-methanoisoxazolo[5,4-*c*]pyridin-5(6*H*)-one (+)-**7**

To a solution of (1*S*,4*R*)-2-azabicyclo[2.2.1]hept-5-en-3-one (+)-**5** (150 mg, 1.37 mmol) in EtOAc (10 mL), dibromoformaldoxime (360 mg, 1.78 mmol) and solid NaHCO₃ (575 mg, 6.85 mmol) were added. The mixture was vigorously stirred for 12 h and the progress of the reaction was monitored by TLC (EtOAc). Water (5 mL) was added and the organic layer was separated and dried over anhydrous Na₂SO₄. The crude material obtained after evaporation of the solvent was purified by column chromatography on silica gel (cyclohexane/EtOAc 1:9) to give an inseparable mixture of the two cycloadducts (+)-**6** and (+)-**7** (266 mg, 84%). The separation of compounds (+)-**6** and (+)-**7** was achieved by preparative chiral HPLC. Wavelength: 220 nm; eluent: *n*-hexane *i*PrOH (6:4); flow rate: 20 mL/min; retention times: (+)-**6**: 4.966 min; (+)-**7**: 6.220 min.

(+)-**6**: Crystallized from *i*PrOH as white prisms; mp: 158 °C; $[\alpha]_D^{20} = +77.0$ ($c = 1.00$ in CHCl₃); $R_f = 0.60$ (EtOAc); ¹H NMR (300 MHz, CDCl₃): $\delta = 1.90$ (d, $J = 10.7$ Hz, 1H, H₈), 2.15

(d, $J = 10.7$ Hz, 1H, H₈), 3.18 (s, 1H, H₇), 3.83 (d, $J = 8.3$ Hz, 1H, H_{3a}), 4.20 (s, 1H, H₄), 5.18 (d, $J = 8.3$ Hz, 1H, H_{7a}), 6.68 (bs, 1H, NH); ¹³C NMR (75 MHz, CDCl₃): $\delta = 36.0, 53.2, 57.7, 65.5, 85.4, 136.6, 177.0$; MS: 230.9 [M+H]⁺. Anal. calcd for C₇H₇BrN₂O₂: C 36.39, H 3.05, N 12.12, found: C 36.26, H 2.98, N 12.02. (+)-7: crystallized from *i*PrOH as white needles; mp: 167 °C; [α]_D²⁰ = +127.1 ($c = 1.00$ in CHCl₃); $R_f = 0.60$ (EtOAc); ¹H NMR (300 MHz, CDCl₃): $\delta = 1.75$ (d, $J = 11.0$ Hz, 1H, H₈), 2.10 (d, $J = 11.0$ Hz, 1H, H₈), 2.90 (s, 1H, H₄), 3.80 (d, $J = 8.3$ Hz, 1H, H_{3a}), 4.12 (s, 1H, H₇), 5.00 (d, $J = 8.3$ Hz, 1H, H_{7a}), 6.52 (bs, 1H, NH); ¹³C NMR (75 MHz, CDCl₃): $\delta = 35.5, 46.9, 58.9, 59.3, 87.8, 138.0, 178.0$; MS: 230.9 [M+H]⁺. Anal. calcd for C₇H₇BrN₂O₂: C 36.39, H 3.05, N 12.12, found: C 36.28, H 2.99, N 12.05.

(3aS,4R,7S,7aR)-3-Bromo-4,5,7,7a-tetrahydro-4,7-methanoisoxazolo[4,5-c]pyridin-6(3aH)-one (-)-6 and (3aR,4S,7R,7aR)-3-bromo-3a,4,7,7a-tetrahydro-4,7-methanoisoxazolo[5,4-c]pyridin-5(6H)-one (-)-7

Compounds (-)-6 and (-)-7 were obtained as described for their enantiomers starting from derivative (-)-5. The separation of compounds (-)-6 and (-)-7 was achieved by preparative chiral HPLC. Wavelength: 220 nm; eluent: *n*-hexane/*i*PrOH (6:4); flow rate: 20 mL/min; retention times: (-)-6: 4.966 min; (-)-7: 8.081 min.

(-)-6: crystallized from *i*PrOH as white prisms; mp: 158 °C; [α]_D²⁰ = -76.8 ($c = 1.00$ in CHCl₃); Anal. calcd for C₇H₇BrN₂O₂: C 36.39, H 3.05, N 12.12, found: C 36.25, H 2.93, N 11.99.

(-)-7: crystallized from *i*PrOH as white needles; mp: 167 °C; [α]_D²⁰ = -126.7 ($c = 1.00$ in CHCl₃); Anal. calcd for C₇H₇BrN₂O₂: C 36.39, H 3.05, N 12.12, found: C 36.23, H 2.89, N 12.00. All the spectroscopic data are identical to those of the corresponding enantiomer.

(3aR,4S,6R,6aS)-3-Bromo-6-carboxy-4,5,6,6a-tetrahydro-3aH-cyclopenta[d]isoxazol-4-aminium methanesulfonate (-)-3

To a solution of compound (+)-6 (100 mg, 0.43 mmol) in THF (13.6 mL), water (30 μ L) and MSA (84 μ L, 1.29 mmol) were added. The reaction mixture was heated at reflux for 24 h. After evaporation of the solvent, the residue was dissolved in water and the solution was submitted to cation-exchange chromatography using Amberlite IR-120 plus.

The acidic solution was slowly eluted onto the resin, and then the column was washed with water until the pH was neutral. The compound was then eluted off the resin with 1 M NH₄OH, and the product-containing fractions were combined and concentrated under vacuum. The residue was treated with 1 equivalent of MSA to afford the desired compound (-)-3 as methanesulfonate salt (133 mg, 90%). Pale yellow oil; [α]_D²⁰ = -29.4 ($c = 0.40$ in H₂O); ¹H-NMR (DMSO-*d*₆, 300 MHz): $\delta = 1.94$ (ddd, $J = 6.8, 8.5, 16.1$ Hz, 1H, H₅), 2.22–2.32 (m, 1H, H₅), 2.30 (s, 3H, CH₃SO₃⁻), 3.02 (ddd, $J = 5.6, 8.5, 8.5$ Hz, 1H, H₆), 3.74–3.82 (m, 1H, H₄), 4.08 (dd, $J = 3.5, 10.0$ Hz, 1H, H_{3a}), 5.32 (dd, $J = 5.6, 10.0$ Hz, 1H, H_{6a}), 8.07 (bs, 3H, NH₃⁺), 12.90 (bs, 1H, COOH); ¹³C NMR (DMSO-*d*₆, 75 MHz): $\delta = 32.7, 40.7, 51.4, 53.4, 62.0, 88.5, 139.7, 174.0$; MS: 249.0 [M+H]⁺. Anal. calcd for C₈H₁₃BrN₂O₆S: C 27.84, H 3.80, N 8.12, found: C 28.02, H 3.87, N 8.02.

(3aS,4R,6S,6aS)-3-Bromo-4-carboxy-4,5,6,6a-tetrahydro-3aH-cyclopenta[d]isoxazol-6-aminium methanesulfonate (+)-4

To a solution of compound (+)-7 (100 mg, 0.43 mmol) in THF (13.6 mL), water (30 μ L) and MSA (84 μ L, 1.29 mmol) were added. The reaction mixture was heated at reflux for 24 h.

The white solid was collected by filtration in pure form as methanesulfonate salt (141 mg, 95%). White solid; mp: dec. >204 °C; [α]_D²⁰ = +20.0 ($c = 0.20$ in H₂O); ¹H NMR (DMSO-*d*₆, 300 MHz): $\delta = 1.85$ (ddd, $J = 10.7, 10.7, 12.6$ Hz, 1H, H₅), 2.22–2.32 (m, 1H, H₅), 2.28 (s, 3H, CH₃SO₃⁻), 3.08 (ddd, $J = 6.6, 6.6, 10.7$ Hz, 1H, H₄), 3.62 (ddd, $J = 5.8, 5.8, 10.7$ Hz, 1H, H₆), 4.28 (dd, $J = 6.6, 10.7$ Hz, 1H, H_{3a}), 5.22 (dd, $J = 5.8, 10.7$ Hz, 1H, H_{6a}), 8.12 (bs, 3H, NH₃⁺), 13.10 (bs, 1H, COOH); ¹³C NMR (DMSO-*d*₆, 75 MHz): $\delta = 32.9, 40.5, 45.8, 57.9, 59.2, 88.3, 141.7, 173.8$; MS: 249.0 [M+H]⁺. Anal. calcd for C₈H₁₃BrN₂O₆S: C 27.84, H 3.80, N 8.12, found: C 27.99, H 3.86, N 8.07.

(3aS,4R,6S,6aR)-3-Bromo-6-carboxy-4,5,6,6a-tetrahydro-3aH-cyclopenta[d]isoxazol-4-aminium (+)-3

Compound (+)-3 was obtained as described for its enantiomer starting from derivative (-)-6. White solid; mp: dec. > 204 °C; [α]_D²⁰ = +30.0 ($c = 0.40$ in H₂O); Anal. calcd for C₈H₁₃BrN₂O₆S: C 27.84, H 3.80, N 8.12, found: C 27.98, H 3.86, N 8.03. All the spectroscopic data are identical to those of the corresponding enantiomer.

(3aR,4S,6R,6aR)-3-Bromo-4-carboxy-4,5,6,6a-tetrahydro-3aH-cyclopenta[d]isoxazol-6-aminium methanesulfonate (-)-4

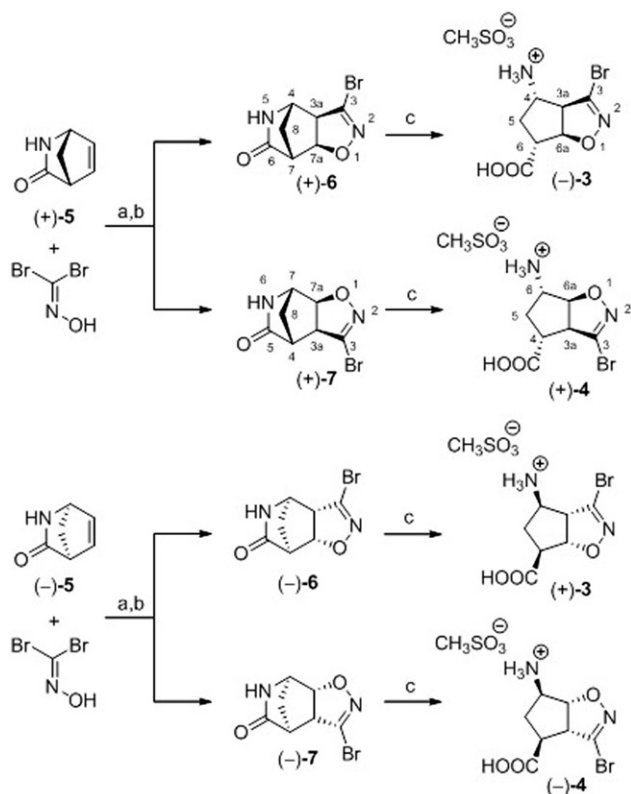
Compound (-)-4 was obtained as described for its enantiomer starting from derivative (-)-7. Pale yellow oil; [α]_D²⁰ = -19.4 ($c = 0.40$ in H₂O); Anal. calcd for C₈H₁₃BrN₂O₆S: C 27.84, H 3.80, N 8.12, found: C 28.00, H 3.87, N 8.01. All the spectroscopic data are identical to those of the corresponding enantiomer.

Protein purification, activity, and inhibition studies

Pig liver GABA-AT was purified as previously described¹⁷. Enzyme activity and residual activity during time- and concentration-dependent inhibition of GABA-AT were assayed essentially as previously described²⁴ with the only modification consisting in the replacement of 100 mM pyrophosphate buffer, pH 8.6, with 100 mM HEPES, pH 8.6. Inactivation reaction was carried out in 30 mM HEPES buffer, pH 7.4, containing 1 mM α -ketoglutarate, as previously reported for inactivation with Vigabatrin¹⁷. Spectrophotometric measurements were carried out on a HP8452 diode array spectrophotometer (Agilent Technologies, Santa Clara, CA).

Molecular modeling

All molecular modeling studies were performed on a MacPro dual 2.66 GHz Xeon running Ubuntu 12.04 (NetBeans, Redwood City, CA). The GABA-AT structure was downloaded from the PDB data bank (<http://www.rcsb.org/> PDB ID: 1OHW). The preparation wizard of the Maestro GUI was used to fix the protein (<http://www.schrodinger.com/Maestro>). Ligand structures were built with the 2D Sketcher of the Maestro GUI and minimized using the MMFF94x forcefield until an RMSD gradient of 0.05 kcal mol⁻¹ Å⁻¹ was reached. Accordingly to scheme 1, PLP was protonated, while the ϵ -amino group of Lys329 was not protonated. The studied adducts had a double protonation on the imine and the pyridine nitrogen atoms. The docking simulations were performed using Plants²⁵ (12 Å radius grid box), and GLIDE²⁶ (10 Å grid box) with the grid center into the centroid of co-crystallized inhibitor coordinates. Covalent docking was performed with PRIME²⁷ using default setting. The images in the manuscript were created with Pymol (The Pymol Molecular



Scheme 2. Reagents and conditions: (a) NaHCO_3 , EtOAc; (b) preparative HPLC separation; (c) $\text{CH}_3\text{SO}_3\text{H}$, H_2O , THF, Δ .

Graphics System, www.pymol.org, DeLano Scientific LLC, San Carlos, CA).

Results and discussion

Synthesis of bicyclic γ -amino acids

The key step in the synthesis of target amino acids (–)-3, (+)-3, (–)-4, and (+)-4 is represented by the 1,3-dipolar cycloaddition of bromonitrile oxide, generated *in situ* by dehydrohalogenation of the stable precursor dibromoformaldoxime (DBF)²⁸, to commercially available (1*S*,4*R*)-2-azabicyclo[2.2.1]hept-5-en-3-one [(+)-5] or its enantiomer (1*R*,4*S*)-[(–)-5], respectively (Scheme 2).

A mixture of the two regioisomeric cycloadducts [(+)-6/(+)-7 and (–)-6/(–)-7] was formed in the 1,3-dipolar cycloaddition reaction. As reported elsewhere, the nitrile oxide attacks exclusively the *exo* face of the dipolarophile^{29–31}. As a matter of fact, the absence of appreciable coupling between the isoxazoline and bridgehead protons is typical of norbornene *exo* adducts³¹. Unfortunately, the two pairs of regioisomeric cycloadducts [e.g., (+)-6 from (+)-7] could not be separated by silica gel column chromatography. Therefore, we evaluated the possibility to separate the two couples of cycloadducts by preparative HPLC. A good separation of regioisomeric cycloadducts (+)-6/(+)-7 ($\alpha = 1.7$; $R_s = 3.1$) and (–)-6/(–)-7 ($\alpha = 3.0$; $R_s = 8.0$) was achieved with a chiral column containing a *tris*-(3,5-dimethylphenyl)carbamoyl amylose as the stationary phase. The ratio between regioisomers 6 and 7 turned out to be 45:55. The structures of the two regioisomers 6 and 7 were secured by comparing their ¹H NMR spectra with those of analogue compounds, previously reported in the literature, whose structures were firmly established by single crystal X-ray analysis³⁰. As in the literature compound, derivative 6 shows proton H_{7a} at lower field than the corresponding proton in compound 7

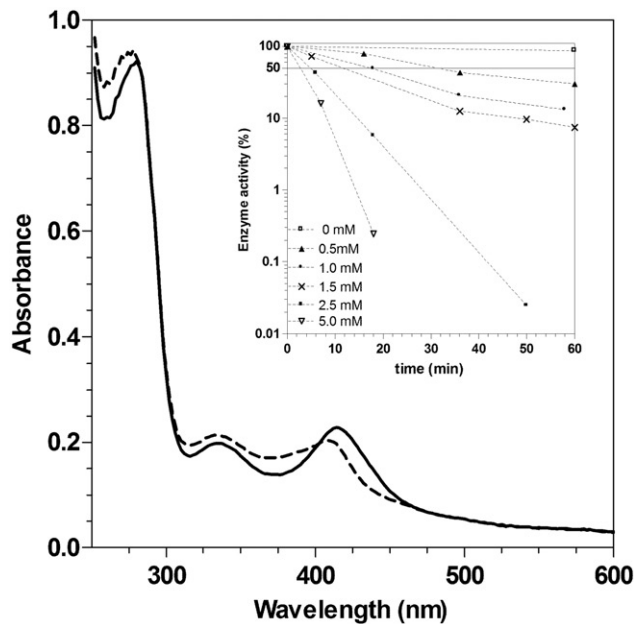


Figure 2. Absorption spectra of GABA-AT before (continuous line) and after (dashed line) 30 min treatment with 1 mM (+)-3 at 20 °C. Inset: time- and concentration-dependent inactivation of GABA-AT at 25 °C by (+)-3.

(H_{7a}: 5.18 ppm for compound 6 versus 5.00 ppm in derivative 7); in both cases the signal appears as a doublet with an identical value of coupling constant ($J = 8.3$ Hz). Moreover, the same trend was observed for proton H₇ in compound 6 (3.18 ppm) in comparison with the corresponding proton H₄ (2.90 ppm) in derivative 7. The synthesis of the final γ -amino acids was accomplished through the hydrolysis of intermediate lactams performed with methanesulfonic acid (MSA) and water in THF at reflux (Scheme 2).

Assay of bicyclic γ -amino acids as GABA-AT inhibitors

The four derivatives (–)-3, (+)-3, (–)-4, and (+)-4 were assayed for their ability to irreversibly inactivate pig liver GABA-AT. This enzyme shares 96/98% sequence identity/similarity with the human enzyme³² and was successfully employed to study the mechanism of inactivation by Vigabatrin¹⁷. In addition, the crystal structures of this same enzyme in the free and Vigabatrin-bound form, both at 2.3 Å resolution, are available for modeling and docking studies^{16,33}.

In a preliminary experiment, all four compounds (1 mM) were tested as GABA-AT inhibitors. Compound (+)-3 proved to significantly inhibit the enzyme (more than 50% inhibition in 30 min at 25 °C). During the course of the reaction, the absorption spectrum changed (Figure 2) with the most significant changes occurring at 425 nm (decrease) and at 376 nm (increase); an isosbestic point at 401 nm was clearly visible. Being the modification of the spectrum of the enzyme a typical indicator of a change in the cofactor chemical state in the active site, this was regarded as the first indication of a reaction occurring at the active site of the enzyme. On the contrary, compound (–)-3 only slightly affected activity and spectrum (data not shown), whereas treatment with either (–)-4 or (+)-4 did not lead to inhibition (Table 1). Following storage at 4 °C, spectra and activity of GABA-AT were recorded at 1 d and 7 d (only spectra) from initial treatment. With respect to the spectroscopic changes observed during the first 30 min of reaction with the four compounds under analysis, no further changes were observed. The percentage of GABA-AT inhibition after incubation for 24 h with the

Table 1. Percentage of inhibition at the screening concentration (1 mM) after 1 d at 4 °C.

Compound	Inhibition (%)
(+)- 3	98
(-)- 3	27
(+)- 4	0
(-)- 4	0

compounds tested at the 1 mM screening concentration is provided in Table 1.

Compound (+)-**3** gave a time- and concentration-dependent inhibition of GABA-AT. The kinetic constants for (+)-**3** at pH 7.4 and at 25 °C were determined using a Kitz and Wilson replot³⁴. The k_{inact} and K_{I} values were found to be 0.251 min⁻¹ and 5.25 mM, respectively, thus resulting in second-order rate constant of inhibition $k_{2\text{nd}} (k_{\text{inact}}/K_{\text{I}}) = 0.048 \text{ min}^{-1} \text{ mM}^{-1}$. According to the latter value, compound (+)-**3** is a much less potent inhibitor towards GABA-AT than CPP-115 ($k_{2\text{nd}} = 5.7 \text{ min}^{-1} \text{ mM}^{-1}$, pH 6.5), and not even a better inhibitor of GABA-AT than (+)-(*S*)-Vigabatrin ($k_{2\text{nd}} = 1.7 \text{ min}^{-1} \text{ mM}^{-1}$ at pH 8.5, $0.11 \text{ min}^{-1} \text{ mM}^{-1}$ at pH 6.5). However, given its specificity in respect to (-)-**3**, (+)-**4**, and (-)-**4**, it is likely that additional chemical modifications might lead to new compounds with increased potency as GABA-AT inhibitors. This is conceivable if one considers that a quite dramatic change in the activity of CPP-115 as GABA-AT inhibitor was observed when fluorine atoms were replaced with chlorines³⁵.

Docking studies of bicyclic γ -amino acids in the GABA-AT active site

In order to gain further insight on the possible mechanism of inactivation of GABA-AT by (+)-**3**, a series of docking experiments, aimed also at establishing the structural basis for the inactivity of (-)-**3**, (-)-**4**, and (+)-**4**, were carried out. The X-ray structure of the covalent Vigabatrin-GABA-AT adduct (PDB ID: 2OHW)¹⁶ was used to run docking calculations. The docking studies were carried out by Plants²⁵ and Glide²⁶ and, to simplify the calculations, adduct **8** (Scheme 1), the (+)-**3**-PLP imine adduct, was assumed as already formed. To test the methods performances, Vigabatrin was docked in the enzyme active site, revealing that the lowest energy poses furnished by Plants and Glide were virtually superimposable with the one observed in the X-ray structure (Figure 1S).

Independently of the software used, the docking analysis revealed a consistent binding mode of adduct **8**. For easier interpretation of the docking results, a comparison between the best energy pose of this adduct and the Vigabatrin-GABA-AT complex was performed and this is shown in Figure 3. Concerning the PLP moieties, they showed a good superimposition, as confirmed also by the retention of the H-bonds between the positively charged pyridine nitrogen and the β -carboxylate of Asp298, as well as those that stabilize the phosphate group. Both the carboxylic functions of the inhibitors were almost superimposable and involved in polar interactions with the guanidinium group of Arg192. The cyclopentaisoxazoline scaffold of compound (+)-**3**, mainly the part including C3, C3a and C4 (for numbering refer to Scheme 1), well resembled the Vigabatrin alkylic part, resulting in a good superimposition between the Vigabatrin vinyl bond and C3-Br bond in (+)-**3**. These two functions were in the right geometry for the nucleophilic attack by the ϵ -amino group of Lys329, although the observed distance between Lys329 and the Vigabatrin Michael acceptor is found to be shorter than the one observed for Lys329 and C3 in (+)-**3**.

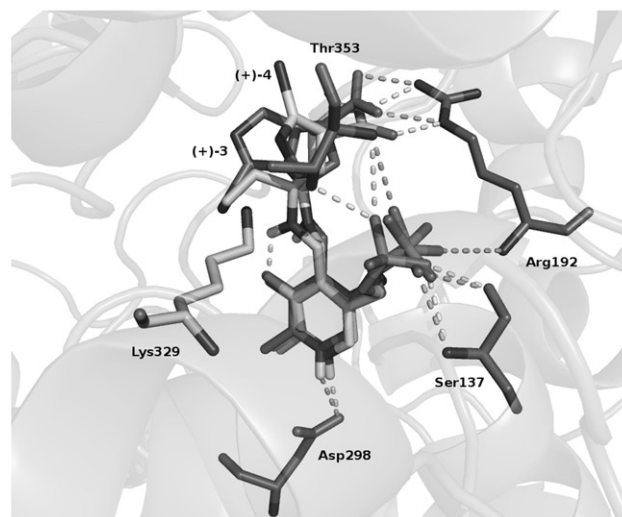


Figure 3. Superposition of co-crystallized Vigabatrin-PLP with proposed binding mode of (+)-**3** (dark gray) and (+)-**4** (light gray) as provided by Plants. H-bonds are shown as dotted lines in light gray for Vigabatrin-PLP, in dark gray for adduct **8**. Lys329, involved in nucleophilic attack, is reported in stick. Distances between ϵ -amino group of Lys329 and the electrophilic center of Vigabatrin and adduct **8** are 2.3 and 2.9 Å, respectively. The main residues involved in binding are also reported.

This is likely due to the docking method, which puts interacting atoms typically at a distance wider than the sum of their van der Waals radii³⁶.

Notably, the docking analysis provides an explanation for the lack of reactivity of compounds (+)-**4** and (-)-**4**: in this case, the electrophilic centre is located too far (more than 4.5 Å) from the ϵ -amino group of Lys329, thus in a conformation prohibited to undergo nucleophilic attack. In addition, with the same analysis, the binding mode of (+)-**3** and (-)-**3** showed no significant differences. In an attempt to rationalize the different biological activities of the latter compounds, and taking into account the proposed mechanism of GABA-AT inhibition, we moved from classical (i.e., non-covalent) to a covalent docking approach, which is supported by Prime²⁷. As shown in Figure 4, the covalent adduct with (+)-**3** does not substantially differ between the poses obtained by Plants and Prime, whereas in the case of the adduct formed with (-)-**3**, the overlap between the poses obtained by classical and covalent docking procedures is rather unsatisfactory.

Thus, compound (+)-**3** was at a distance and in a conformation that favors the attack by Lys329. On the contrary, for compound (-)-**3**, despite carbon C3 is at the right distance, the formation of adduct implies a movement as a whole of the rigid bicyclic nucleus and loss of the polar interaction with Arg192. This observation might account for the observed different biological activities of (+)-**3** and (-)-**3**, being the latter a much worse inhibitor than (+)-**3** (Table 1).

Conclusion

In the present work, we used the 3-Br-isoxazoline as a warhead to inhibit mammalian GABA-AT, based on our previous findings that the 3-Br-isoxazoline ring can react with nucleophilic residues when its moiety is correctly positioned into the active site of a target enzyme, and knowing that it can react with amines, to generate the corresponding 3-amino-isoxazolines. On this basis, we tested the newly synthesized compounds (-)-**3**, (+)-**3**, (-)-**4**, and (+)-**4** (Figure 1) as potential GABA-AT inhibitors. Notably, only compound (+)-**3** was found to be a time- and concentration-dependent inhibitor of GABA-AT, although much less efficient

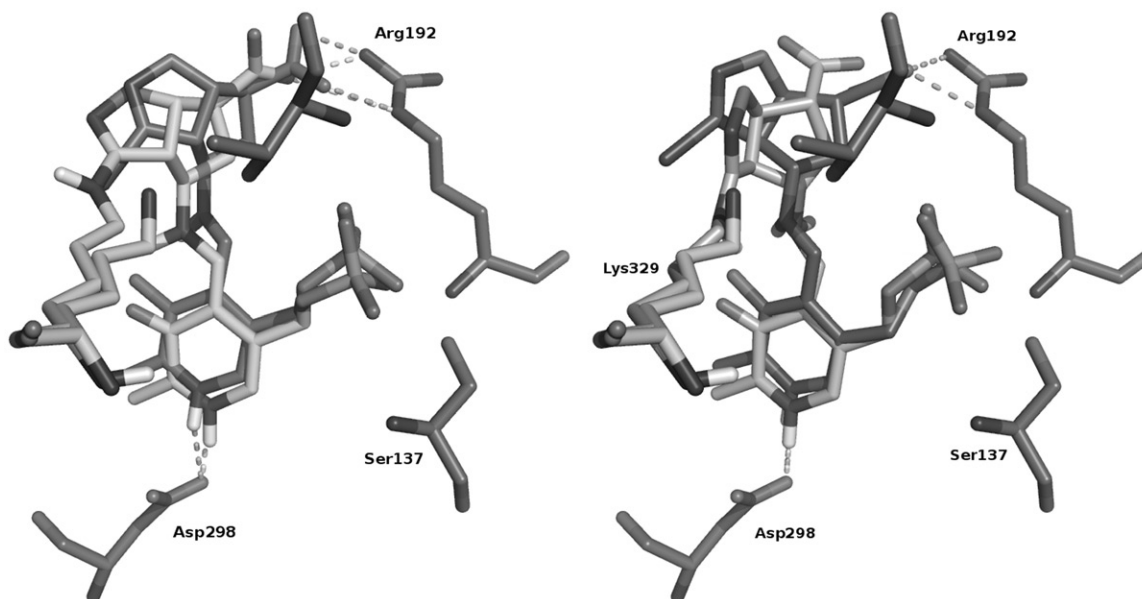


Figure 4. Proposed classical (dark gray) and covalent (light gray) docking binding mode of (+)-3 (left) and (-)-3 (right). H-bonds observed for Plants docking poses are shown as dark dotted lines, whereas for covalent docking poses obtained by Prime²⁷ are shown as light dotted lines.

than Vigabatrin and CPP-115. Docking studies provided a conceivable explanation for the absence of reactivity of the other three isomers tested in this work towards GABA-AT.

This is the first report of 3-Br-isoxazoline derivatives as inhibitors of a PLP-dependent enzyme. Given that some catalytic features are retained in the active site of most of these enzymes, we expect that 3-Br-isoxazoline derivatives, suitably designed to locate in the active site of other PLP-dependent enzymes, might pave the way to the modulation of different metabolic pathways in which these enzymes play key roles.

Acknowledgements

A. C. is grateful to Dr. S. Cosconati for helpful discussion.

Declaration of interests

The authors have declared that no competing interests exist.

Financial support from MIUR to CDM (PRIN 2012) is gratefully acknowledged. DDB thanks Fondazione Roma for partially supporting this work.

References

- Schousboe A, Waagepetersen HS. GABA: homeostatic and pharmacological aspects. *Prog Brain Res* 2007;160:9–19.
- Meldrum BS. GABAergic mechanisms in the pathogenesis and treatment of epilepsy. *Br J Clin Pharmacol* 1989;27:3S–11.
- Fatemi SH. The hyperglutamatergic hypothesis of autism. *Prog Neuro-Psychopharmacol Biol Psychiatry* 2008;32:911 (author reply 912–13).
- Brauns S, Gollub RL, Walton E, et al. Genetic variation in GAD1 is associated with cortical thickness in the parahippocampal gyrus. *J Psychiatr Res* 2013;47:872–9.
- Domschke K, Tidow N, Schrepf M, et al. Epigenetic signature of panic disorder: a role of glutamate decarboxylase 1 (GAD1) DNA hypomethylation? *Prog Neuro-Psychopharmacol Biol Psychiatry* 2013;46:189–96.
- McCarson KE, Enna SJ. GABA Pharmacology: the search for analgesics. *Neurochem Res* 2014;39:1948–63.
- Owens DF, Kriegstein AR. Is there more to GABA than synaptic inhibition? *Nat Rev Neurosci* 2002;3:715–27.
- Ge S, Goh EL, Sailor KA, et al. GABA regulates synaptic integration of newly generated neurons in the adult brain. *Nature* 2006;439:589–93.
- D’Hulst C, Atack JR, Kooy RF. The complexity of the GABAA receptor shapes unique pharmacological profiles. *Drug Discov Today* 2009;14:866–75.
- Blein S, Hawrot E, Barlow P. The metabotropic GABA receptor: molecular insights and their functional consequences. *Cell Mol Life Sci* 2000;7:635–50.
- Borden LA. GABA transporter heterogeneity: pharmacology and cellular localization. *Neurochem Int* 1996;29:335–56.
- Rowley NM, Madsen KK, Schousboe A, White HS. Glutamate and GABA synthesis, release, transport and metabolism as targets for seizure control. *Neurochem Int* 2012;61:546–58.
- Angehagen M, Ben-Menachem E, Ronnback L, Hansson E. Novel mechanisms of action of three antiepileptic drugs, vigabatrin, tiagabine, and topiramate. *Neurochem Res* 2003;28:333–40.
- Mattson RH, Meldrum BS. Vigabatrin. Mechanisms of action. In: Levy RH, ed. *Antiepileptic drugs*. Raven: New York; 1995:903–13.
- Pan Y, Qiu J, Silverman RB. Design, synthesis, and biological activity of a difluoro-substituted, conformationally rigid vigabatrin analogue as a potent gamma-aminobutyric acid aminotransferase inhibitor. *J Med Chem* 2003;46:5292–3.
- Storici P, De Biase D, Bossa F, et al. Structures of gamma-aminobutyric acid (GABA) aminotransferase, a pyridoxal 5'-phosphate, and [2Fe-2S] cluster-containing enzyme, complexed with gamma-ethynyl-GABA and with the antiepilepsy drug vigabatrin. *J Biol Chem* 2004;279:363–73.
- De Biase D, Barra D, Bossa F, et al. Chemistry of the inactivation of 4-aminobutyrate aminotransferase by the antiepileptic drug vigabatrin. *J Biol Chem* 1991;266:20056–61.
- Choi S, Storici P, Schirmer T, Silverman RB. Design of a conformationally restricted analogue of the antiepilepsy drug Vigabatrin that directs its mechanism of inactivation of gamma-aminobutyric acid aminotransferase. *J Am Chem Soc* 2002;124:1620–4.
- Pan Y, Calvert K, Silverman RB. Conformationally-restricted vigabatrin analogues as irreversible and reversible inhibitors of gamma-aminobutyric acid aminotransferase. *Bioorg Med Chem* 2004;12:5719–25.
- (a) Ettari R, Tamborini L, Angelo IC, et al. Development of rhodesain inhibitors with a 3-bromoisoxazoline warhead. *ChemMedChem* 2013;8:2070–6. (b) Ettari R, Pinto A, Tamborini L, et al. Synthesis and biological evaluation of Papain-family cathepsin L-like cysteine protease inhibitors containing a 1,4-benzodiazepine scaffold as antiprotozoal agents. *ChemMedChem* 2014;9:1817–25.
- (a) Tamborini L, Pinto A, Smith TK, et al. Synthesis and biological evaluation of CTP synthetase inhibitors as potential agents for the treatment of African trypanosomiasis. *ChemMedChem*

- 2012;7:1623–34. (b) Conti P, Pinto A, Wong PE, et al. Synthesis and *in vitro/in vivo* evaluation of the antitrypanosomal activity of 3-bromoacivicin, a potent CTP synthetase inhibitor. *ChemMedChem* 2011;6:329–33.
22. Bruno S, Pinto A, Paredi G, et al. Discovery of covalent inhibitors of glyceraldehyde-3-phosphate dehydrogenase, a target for the treatment of protozoal infections. *J Med Chem* 2014;57:7465–71.
23. Girardin M, Alsabeh PG, Lauzon S, et al. Synthesis of 3-aminoisoxazoles via the addition-elimination of amines on 3-bromoisoxazolines. *Org Lett* 2009;11:1159–62.
24. Lippert B, Metcalf BW, Jung MJ, Casara P. 4-Amino-hex-5-enoic acid, a selective catalytic inhibitor of 4-aminobutyric-acid aminotransferase in mammalian brain. *FEBS J* 1977;74:441–5.
25. Korb O, Stutzle T, Exner TE. Empirical scoring functions for advanced protein-ligand docking with PLANTS. *J Chem Inf Model* 2009;49:84–96.
26. Glide, version 5.5. New York, NY: Schrödinger, Inc.; 2009.
27. Prime, version 2.1. New York, NY: Schrödinger, LLC; 2009.
28. (a) Pinto A, Conti P, De Amici M, et al. Synthesis and pharmacological characterization at glutamate receptors of the four enantiopure isomers of tricholomic acid. *J Med Chem* 2008;51:2311–15. (b) Pinto A, Conti P, De Amici M, et al. Synthesis of enantiomerically pure HIP-A and HIP-B and investigation of their activity as inhibitors of excitatory amino acid transporters. *Tetrahedron: Asymmetry* 2008;19:867–75. (c) Pinto A, Conti P, Tamborini L, De Micheli C. A novel simplified synthesis of acivicin. *Tetrahedron: Asymmetry* 2009;20:508–11.
29. Katagiri N, Yamatoya Y, Ishikura M. The first synthesis of a 2',3'-methano carbocyclic nucleoside. *Tetrahedron Lett* 1999;40:9069–72.
30. (a) Memeo MG, Bovio B, Quadrelli P. RuO₄-catalyzed oxidation reactions of isoxazolino-2-azanorbornane derivatives: a short-cut synthesis of tricyclic lactams and peptidomimetic γ -aminoacids. *Tetrahedron* 2011;67:1907–14. (b) Memeo MG, Mantione D, Bovio B, Quadrelli P. RuO₄-catalyzed oxidation reactions of *N*-alkylisoxazolino-2-azanorbornane derivatives: an expeditious route to tricyclic γ -lactams. *Synthesis* 2011;13:2165–74.
31. Quadrelli P, Mella M, Paganoni P, Caramella P. Cycloadditions of nitrile oxides to the highly reactive *N*-acyl-2-oxa-3-azanorborn-5-enes afford versatile cycloadducts and a convenient entry to highly functionalized derivatives. *Eur J Org Chem* 2000;14:2163–620.
32. De Biase D, Barra D, Simmaco M, et al. Primary structure and tissue distribution of human 4-aminobutyrate aminotransferase. *FEBS J* 1995;227:476–80.
33. Storici P, Capitani G, De Biase D, et al. Crystal structure of GABA-aminotransferase, a target for antiepileptic drug therapy. *Biochemistry* 1999;38:8628–34.
34. Kitz R, Wilson IB. Esters of methanesulfonic acid as irreversible inhibitors of acetylcholinesterase. *J Biol Chem* 1962;237:3245–9.
35. Yuan H, Silverman RB. Structural modifications of (1*S*,3*S*)-3-amino-4-difluoromethylenecyclopentanecarboxylic acid, a potent irreversible inhibitor of GABA aminotransferase. *Bioorg Med Chem Lett* 2007;17:1651–4.
36. Burgi HB, Dunitz JD. From crystal statics to chemical dynamics. *Acc Chem Res* 1983;16:153–61.

Supplementary material available online
Supplementary Figure 1S.